The Relationship Between Galaxy Orientation within Galaxy Clusters and Filaments of Dark Matter in the Deep Lens Survey (DLS)

E.Q. Finney, advised by D. Wittman

September 10, 2012

Abstract

Despite a growing understanding of the large-scale structure of the Universe, little is known about the interactions between the galaxies that comprise the different substructures (filaments, sheets, clusters, voids). Observational and numerical studies have raised questions about whether galaxies are preferentially oriented in certain directions, and if such orientation exists, whether it is in any way related to the proximity of filaments of galaxies. Using DLS data, we analyzed the orientations of galaxies with respect to the axes of presumed filaments, examining general trends of orientation patterns. No statistically significant results were found in the overall analysis, although future work will be conducted to determine the behavior of galaxies at different angles or distances from the filament, red and blue galaxies, and galaxies with differing radii from the center of the cluster, as well as the redshift evolution of orientation patterns.

1 Introduction

The past twenty years have seen a remarkable increase in our understanding of the structure of the Universe, lending strong evidence for the existence of filaments of dark matter between galaxy clusters and producing viable models concerning their interactions with nearby galaxies. Observational and numerical evidence strongly point to a "cosmic web" substructure of the Universe, with high-density clusters of dark and luminous matter connected by filaments of galaxies and dark matter, and large low-density voids separating these structures (Pimbblet et al. 2004; Altay et al. 2006; Colberg et al. 2005; Pimbblet 2005; Aragón-Calvo et al. 2010). These studies also lend evidence that cosmic web structures can influence the orientations of cluster substructures in close proximity. In particular, several numerical studies suggest that dark matter haloes within galaxy clusters tend to align toward nearby intercluster filaments (Altay et al. 2006; Jing 2002; Bailin & Steinmetz 2005; among others).

A possible explanation for this behavior was proposed by West (1993), who suggested that the properties and orientations of galaxies in clusters (as well as the properties/orientations of the clusters themselves) could be explained by a model in which galaxies merge with clusters in preferred directions. His work, which looked at numerical simulations as well as observations of high-frequency radio galaxies, popularized the notion of anisotropic hierarchical merging of galaxies and galaxy clusters along intercluster filaments of dark matter. Other numerical simulations (Altay et al. 2006; Pereira et al. 2008; Pimbblet 2005; Aragón-Calvo et al. 2010; Colberg et al. 2005) support this hypothesis. Recent observational studies connect galaxy alignment within clusters to this model of anisotropic merging of galaxies with galaxy clusters, although several studies note mixed results and suggest that galaxy color (Tempel et al. 2012; Kodama et al. 2001; Faltenbacher et al. 2007) or dynamical age (Plionis & Basilakos 2002; Plionis et al. 2003; Plionis 2004; Faltenbacher et al. 2007) may affect the signal of galaxy alignment.

Despite the broad scope of these studies, they have many limitations that prevent them from adequately explaining the interactions between galaxy clusters and filaments in close proximity to each other. Most of these studies are limited to a relatively small number of low-redshift galaxy clusters. Moreover, although extensive discussion of simulated cluster substructure has occurred, very few studies have examined how fil-

aments of galaxies particularly affect the alignments of galaxies in clusters, a question that profoundly influences any research that utilizes weak gravitational lensing. If galaxies are indeed aligned relative to nearby filaments and clusters, the assumptions of random galaxy orientation inherent in weak gravitational lensing studies would have to be reconsidered.

In this work, we examine the orientations of galaxies within hundreds of galaxy clusters to determine how these orientations may be affected by infall from filaments. This work is organized in the following manner: Section 2 begins by describing the data used and how the catalogs of data were created. The next section (Section 3) explains how these data were analyzed in order to rotate them along the direction of the intercluster filament. Our results are detailed in Section 4, and Section 5 discusses these results in the larger context of current research and points to future work. Finally,the paper is concluded with a summary (Section 6).

2 Observations from the Deep Lens Survey

In the interest of investigating these questions, we used the Deep Lens Survey (DLS) to obtain observational data of galaxy clusters. The DLS, a survey of five $2^\circ \times 2^\circ$ fields, was originally designed to promote study of weak gravitational lensing, so each field had 54 ksec exposure time (12 ksec in *BV z'*; 18 ksec in *R*). This feature of the survey ensured that the data obtained had very well-measured shapes, a necessary detail in any project that focuses on the ellipticity components of the galaxies it seeks to examine. Additionally, it allowed the DLS to collect significant information about high-redshift galaxy clusters (up to 19mag/arcsec^2 in *BV R* and 28mag/arcsec^2 in *z'*). Redshifts were collected as photometric probability distribution functions rather than using spectroscopic data. For these reasons, the DLS seemed ideal for this particular project.

The fields of the DLS were chosen without consideration of known features or targets, but with the intent of avoiding bright stars or areas with strong extinction; in this sense, they were "random" and could be considered representative of low-extinction, unmasked regions of the sky. Data were collected using Mosaic, a CCD camera with a 35' field. The data analysis found in this work was performed on catalogs of galaxies and of galaxy clusters that had been created prior to the beginning of this study. In this work, we use galaxy catalogs created by the SExtractor (version 2.1.6, developed by the DLS collaboration), using data obtained from the DLS.

Because of the very large number of galaxies involved in the DLS, collecting spectroscopic galaxy redshift information was beyond the scope of this survey. Thus, redshifts were collected as photometric probability distribution functions rather than using spectroscopic data. In addition to this practical reason for collecting photometric redshift information, use of photometric redshifts would be more feasible when attempting to gather information about high-redshift objects, a crucial component of the DLS.

In order to be included in the catalog, all galaxies were required to meet certain criteria. All galaxies in the catalog were between 22$^{\text{nd}}$ and 25$^{\text{th}}$ magnitudes in the *R* band. Ellipticity components were measured with respect to the sky, with the standard notation of the +x coordinates to the right, +y coordinates up, and with right ascension (RA, a measure of the horizontal position of a star in the sky) heading in the -x direction and declination (Dec, a measure of the vertical position of a star in the sky) in the +y direction. Any galaxy whose uncertainty in the ellipticity value ($\Delta\varepsilon$) exceeded 0.3 was considered poorly measured and was thus eliminated from the galaxy catalog, as were galaxies so masked by a foreground object as to make running the SExtractor prohibitive.

The DLS cluster catalogs, comprised of 780 cluster candidates with redshifts extending back to z=1.2, were created using a Bayesian cluster-identifying algorithm developed by Ascaso, Wittman & Benítez (2012). The algorithm determines the probability that any galaxy in a survey is the brightest cluster galaxy (BCG) in a cluster, and hence the probability that a galaxy cluster is centered approximately at that galaxy. Thus, the algorithm went through a field, calculating the probability that a cluster could be centered on a given galaxy given the properties of the galaxy (position, photometric redshift, magnitude, spectral type) and known cluster information such as the "cluster luminosity function, density profiles, and photometric redshift distribution." (Ascaso et al. 2012, hereafter referred to as AWB 2012) A background probability level is computed and then galaxies with probability of cluster membership 3-σ greater than the background probability are included as cluster members and used to compute density, richness (Λ_{cl}), luminosity (L_{cl}), redshift, etc. Cluster redshift was then estimated by using the highest-probability redshift slice

in a clusters's photometric redshift probability distribution function, as determined by the Bayesian cluster finder. The RA and Dec of the cluster were then determined to be located at the position of the brightest galaxy within that redshift band and within 1.5Mpc of the (hypothesized) cluster center. Luminosity and mass of the clusters were calculated using the cluster richness parameter (Λ_{cl}), as described in AWB 2012. All of these quantities were measured using the galaxy catalog created by the DLS collaboration.

3 Working With the Clusters

3.1 *Refining the estimate for the location of the centers of the clusters*

A good estimate of the three-dimensional location of the cluster centers is crucial to understanding galaxy orientation in this study, and masking from foreground objects may skew these estimates. Thus, the previously created cluster catalogs were further refined by determining the fraction of the cluster that was unmasked and eliminating any cluster with a fraction unmasked < 0.85. This condition was decided upon because when a test catalog of 10000 galaxies from the second field (F2) was used, the entire field was approximately 85% unmasked and 6 of 128 clusters (4.7%) were more masked than the overall field, as shown in Figure 1.

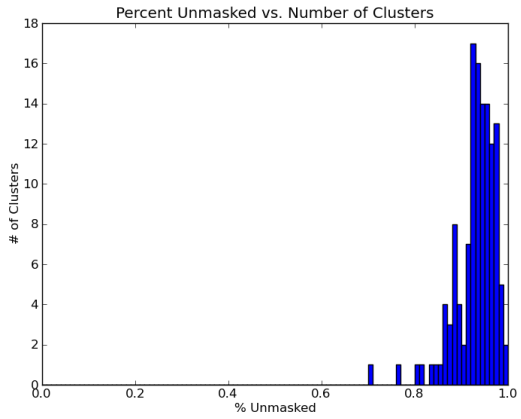

Figure 1: Nearly all galaxy clusters were over 85% unmasked.

The cluster centers in the DLS had been previously identified and their centers approximated using the algorithm of AWB 2012, but in this method these clusters were then subjected to a re-centering process in an effort to establish more accurate cluster centers. The overall process relies on the assumption that the visible galaxies that comprise the cluster will be the primary factors in determining the center of mass of a cluster. To this effect, for each cluster identified in the Ascaso DLS catalogs, a smaller catalog of galaxies potentially contributing to the cluster was created and analyzed. To create the catalog, the distance between each galaxy in the field (whose RA and Dec were taken from the galaxy catalog) and the previously estimated cluster center was calculated; if the galaxy's projected distance from the cluster center fell within the projected distance of the virial radius (r_{200}) plus a user-determined buffer (we used a 10% buffer), the galaxy was included in the catalog of galaxies to be further considered as potential cluster members.

Although galaxies beyond a certain point were removed from analysis, other galaxies may be included in the cluster catalog despite having a low probability of cluster membership. Thus, calculating a probability of membership based on redshift and projected distance from the cluster center can help to determine the degree to which a given galaxy influences the overall cluster center of mass. In order to avoid unnecessarily eliminating data by simply removing the less likely galaxies, candidates are assigned weights based on their likelihood of being cluster members, a process described in the following paragraphs.

Redshift weights were assigned by assuming that the redshift probability distribution function of the cluster is Gaussian, with a mean at the redshift given by the Ascaso catalogs and a standard deviation given by the error of the redshift (also from the Ascaso catalogs). The galaxy redshift probability distribution function was given by the photometric redshifts from the galaxy catalog. We then wish to ascertain the probability that the galaxy and cluster probability distributions are roughly the same (or at least consistent with each other). To do so, we convolve the distributions using the following relationship, where z_g is the redshift probability distribution function (pdf) of the galaxy, z_{cl} is the pdf of the cluster, Δz is the redshift width of the cluster, $p(f(y))$ is the probability of the cluster's occurring at any given redshift, and $p(g(y))$ is the probability of the galaxy's occurring at any given redshift:

$$w_z = P(z_g = z_{cl}) = \Delta z \int_{-\infty}^{\infty} p(f(y)) \cdot p(g(y))\, dy.$$

Since we are dealing with discrete redshift bins, we must in actuality use the relationship

$$w_z = P(z_g = z_{cl}) = \Delta z \sum_{z=0}^{\infty} p(f(z)) \cdot p(g(z)),$$

where w_z, z_g, z_{cl} and Δz are defined as in the previous equation, $p(f(z))$ is the probability of the cluster's occurring at any given redshift bin, and $p(g(z))$ is the probability of the galaxy's occurring at any given redshift bin. This is essentially equivalent to taking the inner product of the same-sized probability distribution functions and multiplying by the width of the redshift bin. The result gives the probability of the galaxy's redshift distribution being consistent with that of the cluster (ie, the probability that the galaxy is a member of the cluster, given the redshift distributions).

Weights were also necessary to determine the probability of a galaxy's being part of a cluster based on projected distance from the cluster center; although clusters beyond a certain point were eliminated from analysis, their probabilities still matter. These weights were also calculated with the assumption that galaxy density of the cluster would be Gaussian, with a mean radius of zero. Thus, the distance to the center of the cluster was calculated in the same manner as was used to find the abbreviated cluster catalog. Weight (w_{rad}) was then determined by the bell curve function:

$$w_{rad} = e^{-\frac{(d^2)}{(2\sigma^2)}},$$

where d is the projected distance from the galaxy center to the cluster center, and σ is the cluster's r_{200}.

Weights that indicate likelihood of cluster membership are not the only relevant means by which galaxy information should be multiplied. Center of mass calculations require knowledge of the mass of the constituents of the system, and although the galaxy catalog did not include mass information, by assuming a linear relationship between mass and luminosity in galaxies, mass could be estimated. To simplify this process, only the R-band magnitude (R_{mag}) was considered in estimating the mass of each galaxy. Thus, galaxies with a higher R-band magnitude were given higher "luminosity weights" ($lum = 10^{-R_{mag}}$), and likewise galaxies less luminous in the R-band were considered as being less massive and thus having less influence on the center of mass of the cluster.

The assigned weights w_i were then multiplied to find the total weight to apply to the galaxy within the cluster, and then the RA, Dec, and Z of the center of the cluster were calculated in the following manner:

$$\alpha_{cl} = \langle w_i \cdot \alpha_i \rangle$$

$$\delta_{cl} = \langle w_i \cdot \delta_i \rangle$$

$$Z_{cl} = \langle w_i \cdot Z_i \rangle.$$

To ascertain that these centroid calculations were self-consistent, the process was iterated until the results began to converge on a centroid value (ie, the projected radius of the most recently calculated centroid was within 1% of r_{200}, and the redshift value was within 1% of the last redshift calculated). These values were used to create a new cluster catalog with adjusted cluster centers (hopefully more accurate ones). The previously mentioned buffer zone minimized the need to re-extract galaxies from the catalog each time the re-centering process was iterated.

3.2 *Determining the location of the filaments*

After these steps were taken to re-center the clusters, the cluster pairs likely to support filaments of dark matter were identified and a separate catalog of cluster pairs created. Using the data obtained in the numerical study of Colberg et al. (2005), it was evident that about 85% of the all clusters within 10 Mpc/h of each other had a straight filament between them (a result confirmed observationally by Pimbblet et al. 2004). Clusters were assumed to be distinct if they were at least 2 Mpc/h from each other. Thus, any clusters separated by a physical three-dimensional distance between 2 and 10 Mpc/h were noted as cluster pairs likely to have straight and on-center intercluster filaments (see Figure 2), and were separated and placed in the cluster pair catalog. Factors such as cluster photometric redshift error and the error associated with filaments that are straight but not necessarily on-center were not considered for this study; later research may refine these aspects and determine to what degree these errors significantly affect the data analysis.

3.3 *Rotating the clusters to align with the filament axis*

Once a cluster pair catalog was created, in order to combine the data from the clusters, each cluster needed to be rotated into a cluster-centric coordinate system such that the filament axis (which was determined to be the

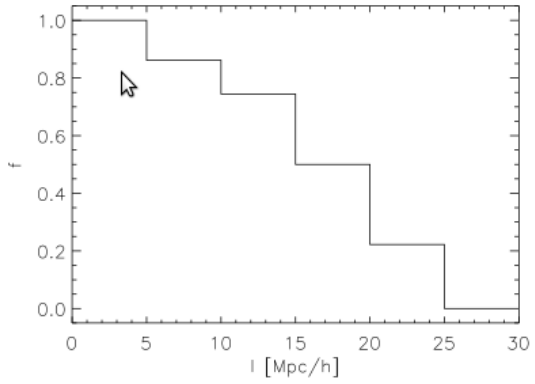

Figure 2: Likelihood of finding a filament between clusters at certain distances. (Colberg et al. 2005)

axis between the center of the two clusters in the cluster pair) would correspond with the y-axis of the system. This rotation was effected by finding the difference between the RA and Dec of the two clusters in the pair and then determining the angle to rotate the cluster so that the filament presumed to exist there would align with the y-axis:

$$\arctan\theta - \frac{\pi}{2},$$

where θ is the angle between the y-axis of the cluster and the filament. This angle was calculated and a rotation matrix was applied to all galaxies in the cluster catalog, as demonstrated in Figure 3. Thus, the analysis may now be continued in a cluster-centric, filament-aligned reference frame.

The angle between each galaxy and the filament axis of the cluster was noted, as were galaxy redshift and radial weights, in order to be used further during the analysis.

Finally, to determine the presence or absence of intrinsic alignment, the galaxies' ellipticity components were converted into the ellipticity components associated with the reference frame of the rotated cluster using double-angle formulas. Δx represents change in Dec, Δy represents change in RA, Δr is total projected separation, and ϕ is the angle between the galaxy location and the x-axis:

$$\cos(2\phi) = \frac{\Delta x^2 - \Delta y^2}{\Delta r^2}$$

$$\sin(2\phi) = \frac{\Delta x - \Delta y}{\Delta r^2}.$$

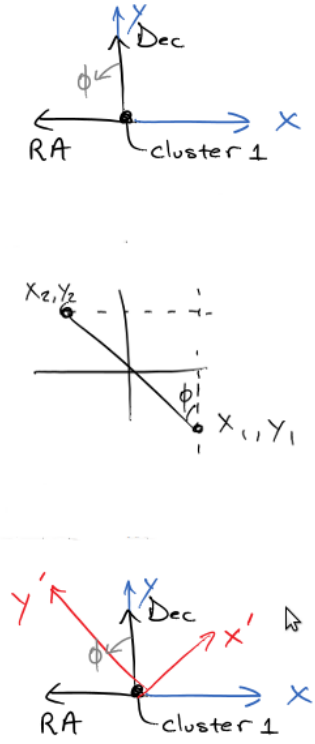

Figure 3: The angle about which the cluster and filament are rotated. Projected coordinates are used to rotate the cluster such that its y-axis aligned with the presumed filament.

These steps were repeated with the second cluster in the pair.

4 Results and Data Analysis

From the way the ellipticity components were calculated, a completely random distribution of galaxy orientations would have a weighted mean of zero for both ellipticity measurements. In order to conduct the analysis of the overall galaxy orientation patterns across each field, information saved during the galaxy rotation steps was used to calculate the weighted averages and weighted standard errors of the mean for each field. Because the curves seemed to demonstrate a non-normal distribution (as shown in Figure 4), a test was conducted to determine normality. In all five fields, there was under a 10% probability that the curves were normal, and thus tests that assume normality, such as t-tests, could not be applied to these data. However, statistical tests that assume nothing but continuous data distribution could be relevant.

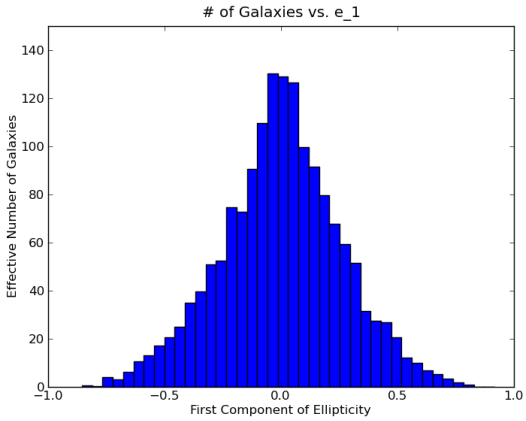

Figure 4: The shape of the weighted histogram for the first ellipticity component (Field 2); the distribution has too little skew to be normal.

In the interest of using a statistical test valid for any continuous distributions of data, two-sample Kolmogorov-Smirnov (KS) statistical tests were used to determine the probability that the data set from each field was centered about zero. The results of these tests, as presented in Tables 1-4 in the Appendix, do not give any reason to suspect a non-random galaxy alignment pattern within galaxy clusters.

To test the code used to rotate the galaxy information and to run the statistical analysis, a galaxy catalog with strong alignment was created and run through the method described above. The deviation from a random distribution was very statistically significant, as demonstrated in Figures 5 and 6.

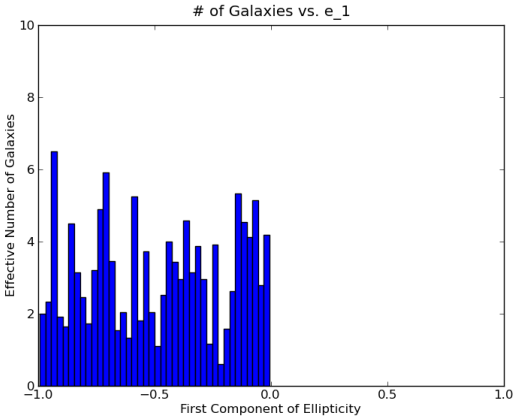

Figure 5: The first ellipticity component of the simulation catalog, with a clearly nonzero mean.

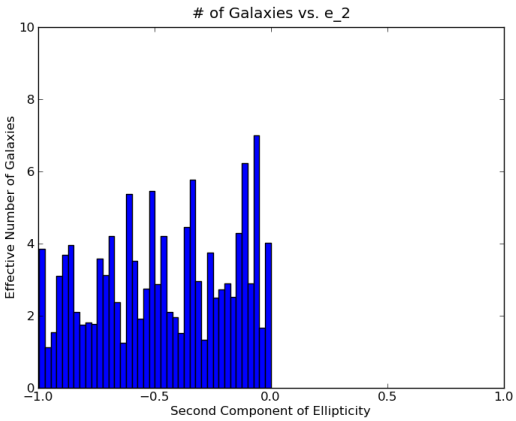

Figure 6: The second ellipticity component of the simulation catalog, also with a clearly nonzero mean.

Determining whether or not galaxies were more likely to be located along the cluster axis was another goal of this study. In order to decide this, a KS test was conducted, comparing the weighted histogram of effective number of galaxies vs. angle to the filament axis to a uniform distribution of galaxies along all filament

angles (this graph is shown in Figure 7). No statistically significant deviation from uniform was discovered in any of the fields - when a chi-squared goodness-of-fit test was applied to the fields, all yielded $> 99\%$ probability of being uniform.

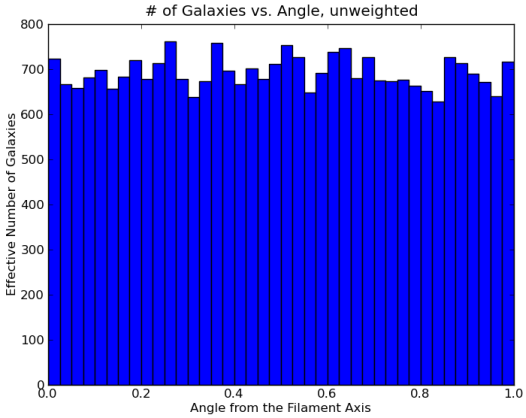

Figure 7: The weighted histogram of effective number of galaxies vs. angle to the filament axis (Field 2). There is no statistically significant deviation from uniform.

All tests were conducted on two catalogs per field – the first catalog included all cluster galaxies, and the second included all cluster galaxies with the inner 250 Mpc/*h* removed to prevent noise from the center of the cluster. However, no significant differences were detected between the two catalogs in any of the fields, as demonstrated in Figures 8-11.

5 Discussion

Hawley and Peebles (1975) first noted clear, if weak, evidence for the radial alignment of galaxies within galaxy clusters, which was later confirmed by several different observational studies (Djorgovski 1983; Agustsson & Brainerd 2006; Jones et al. 2010; Pereira & Kuhn 2005; Pereira & Bryan 2010), although evidence for radial alignment has not always been favorable (Torlina et al. 2006, Trevese & Cirimele 1992). Numerical simulations of the effects of filaments of dark matter on galaxy clusters have also produced results suggesting the possibility of radial alignment of cluster substructures (Catelan et al. 2000; Croft & Metzler 2000; Pereira et al. 2008; Altay et al. 2006).

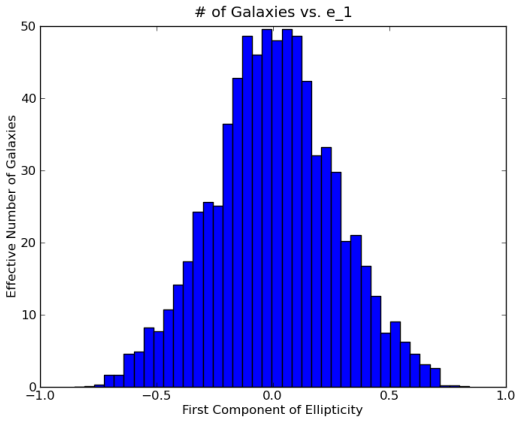

Figure 8: The distribution for the first ellipticity component of Field 3, with center galaxies included.

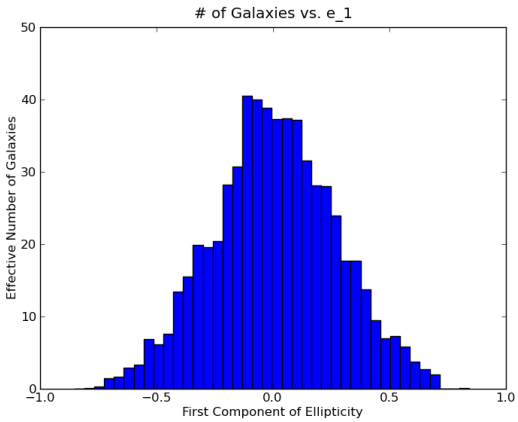

Figure 9: The distribution for the first ellipticity component of Field 3, without center galaxies included.

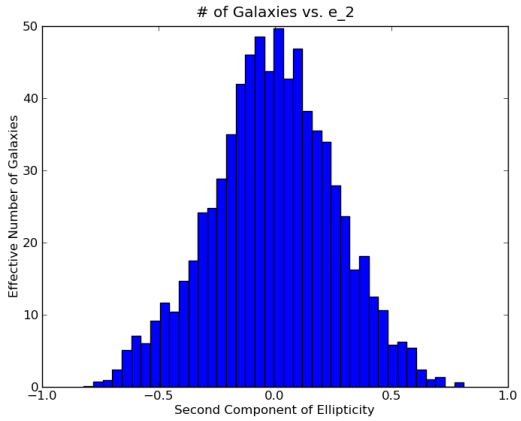

Figure 10: The distribution for the second ellipticity component of Field 3, with center galaxies included.

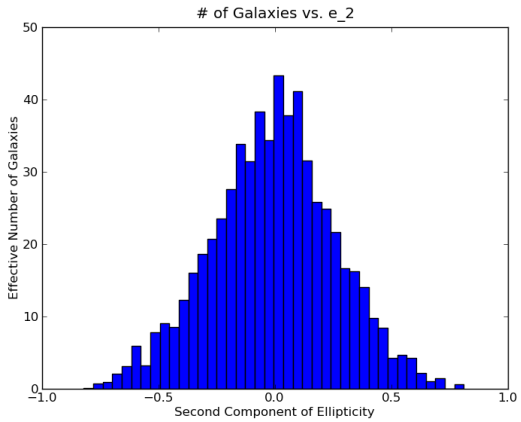

Figure 11: The distribution for the second ellipticity component of Field 3, without center galaxies included.

It is evident that if such an alignment exists, it would strongly affect research that seeks to use weak graviational lensing to understand dark energy and dark matter, and that assumes random galaxy alignment in all images except those distorted by massive foreground objects. This work's findings suggest that at least in the overall population of galaxies examined by the DLS, there is no galaxy alignment that would cast doubt on this assumption.

However, while there is no reason to suspect overall alignments of galaxy orientation with a nearby filament, factors such as a galaxy's angle or distance from the filament, distance from the cluster center, galaxy color, or cluster dynamical age and/or redshift may contain alignment patterns overlooked by a more general analysis. Thus, it would be valuable for future work to examine what orientation patterns, if any, occur in catalogs filtered by these categories.

This work also remains incomplete in that it has not yet examined how errors (such as uncertainties in redshift measurements or center estimates) may affect the results present. Moreover, in order to more rigorously validate these findings, they would have to be compared to cosmological simulations. I hope to pursue this work more thoroughly in the future.

6 Summary

An understanding of galaxy alignment patterns, if such patterns exist, is crucial for determining which assumptions weak gravitational lensing researchers may validly make. Studies of galaxy alignment, both observational and numerical, have produced mixed results concerning whether intrinsic galaxy orientations exist. In order to further probe this question, this study analyzed the orientations of 780 galaxy clusters and over one million galaxies, and thus far has found no statistically significant intrinsic galaxy alignment. Although the study is by no means complete, its results already have implications for dark energy and galaxy evolution research.

Acknowledgements

I would like to thank Dr. Dave Wittman for mentoring me during this summer, Will Dawson for working closely with me to develop ideas and code and to provide solid support, the UC Davis observational cosmology group for fostering a welcoming work atmosphere,

Dr. Rena Zieve for organizing the UC Davis REU program and for offering excellent advice for a future in the field of physics, UC Davis for hosting the REU program, and the NSF for funding this summer's research.

References

[1] Agustsson, I. & Brainerd, T.G. 2006, ApJ, 644, L25.

[2] Altay, G., Colberg, J.M. & Croft, R.A.C. 2006, MNRAS, 370, 1422.

[3] Aragón-Calvo, M.A., van de Weygaert, R. & Jones, B.J.T. 2010, MNRAS, 408, 2163.

[4] Ascaso, B., Wittman, D. & Benítez, N. 2012, MNRAS, 420, 1167.

[5] Bailin, J. & Steinmetz, M. 2005, ApJ, 627, 647.

[6] Colberg, J.M., Krughoff, K.S. & Connolly, A.J. 2005, MNRAS, 359, 272.

[7] Djorgovski, S. 1983, ApJ, 274, L7.

[8] Faltenbacher, A., Li, C., Mao, S., van den Bosch, F.C., Yang, X., Jing, Y.P., Pasquali, A. & Mo, H.J. 2007, ApJ, 662, L71.

[9] Hawley, D.L. & Peebles, P.J.E. 1975, Astronomical Journal, 1434, 477.

[10] Jing, Y.P. 2002, MNRAS, 335, L89.

[11] Jones, B.J.T., van de Weygaert, R. & Aragón-Calvo, M.A. 2010, MNRAS, 408, 897.

[12] Kodama, T., Smail, I., Nakata, F., Okamura, S. & Bower, R.G. 2001, ApJ, 562, L9.

[13] Pereira, M.J. & Bryan, G.L. 2010, ApJ, 721, 939.

[14] Pereira, M.J., Bryan, G.L. & Gill, S.P.D. 2008, ApJ, 672, 825.

[15] Pereira, M.J. & Kuhn, J.R. 2005, ApJ, 627, L21.

[16] Pimbblet, K.A. 2005, MNRAS, 358, 256.

[17] Pimbblet, K.A., Drinkwater, M.J. & Hawkrigg, M.C. 2004, MNRAS, 354, L61.

[18] Plionis, M. & Basilakos, S. 2002, MNRAS, 329, L47.

[19] Plionis, M., Benoist, C., Maurogordato, S., Ferrari, C. & Basilakos, S. 2003, ApJ, 594, 144.

[20] Plionis, M. 2004, IAU Colloquium No. 195.

[21] Tempel, E., Stoica, R.S. & Saar, E. 2012, MNRAS, 000, 1.

[22] Torlina, L., De Propris, R. & West, M.J. 2006, ApJ, 660, L97.

[23] Trevese, D. & Cirimele, G. 1992, Astronomical Journal, 104, 935.

[24] West, M.J. 1993, MNRAS, 268, 79.

[25] West, M.J., Jones, C. & Forman, W. 1995, ApJ, 451, L5.

Appendix

Note that due to incomplete masking information in Fields 1 and 5, these fields could not be completely analyzed, so only the data from Fields 2, 3, and 4 are presented here.

Table 1: Summary Information, First Ellipticity Component, without Centers

	Field 2	Field 3	Field 4
Prob. of Normal Dist.	0.196	0.131	0.151
Weighted Average	0.000173	0.00618	-0.00264
Weighted SEM	0.00990	0.0109	0.0108
Prob. of Center at Zero	1.0	0.767	0.870

Table 2: Summary Information, Second Ellipticity Component, without Centers

	Field 2	Field 3	Field 4
Prob. of Normal Dist.	0.0196	0.0555	0.151
Weighted Average	0.00180	-0.00766	0.00195
Weighted SEM	0.00988	0.0112	0.0109
Prob. of Center at Zero	0.998	0.405	0.995

Table 3: Summary Information, First Ellipticity Component, with Centers

	Field 2	Field 3	Field 4
Prob. of Normal Dist.	0.212	0.158	0.153
Weighted Average	0.00249	0.00391	-0.00264
Weighted SEM	0.00974	0.0112	0.0111
Prob. of Center at Zero	0.919	0.960	0.913

Table 4: Summary Information, Second Ellipticity Component, with Centers

	Field 2	Field 3	Field 4
Prob. of Normal Dist.	0.0538	0.00955	0.0617
Weighted Average	0.00556	-0.00820	0.00343
Weighted SEM	0.0101	0.0117	0.0112
Prob. of Center at Zero	0.259	0.266	0.707